

Analyst

Accepted Manuscript



This is an *Accepted Manuscript*, which has been through the Royal Society of Chemistry peer review process and has been accepted for publication.

Accepted Manuscripts are published online shortly after acceptance, before technical editing, formatting and proof reading. Using this free service, authors can make their results available to the community, in citable form, before we publish the edited article. We will replace this *Accepted Manuscript* with the edited and formatted *Advance Article* as soon as it is available.

You can find more information about *Accepted Manuscripts* in the [Information for Authors](#).

Please note that technical editing may introduce minor changes to the text and/or graphics, which may alter content. The journal's standard [Terms & Conditions](#) and the [Ethical guidelines](#) still apply. In no event shall the Royal Society of Chemistry be held responsible for any errors or omissions in this *Accepted Manuscript* or any consequences arising from the use of any information it contains.

COMMUNICATION

Ratiometric Detection of Oligonucleotide Stoichiometry on Multifunctional Gold Nanoparticles by Whispering Gallery Mode Biosensing†

Cite this: DOI: 10.1039/x0xx00000x

Received 00th January 2012,
Accepted 00th January 2012F. C. Wu,^{a,b,c} Y. Wu,^c Z. Niu^a and F. Vollmer^{c,d*}

DOI: 10.1039/x0xx00000x

www.rsc.org/

A label-free method is developed to ratiometrically determine the stoichiometry of oligonucleotides attached to the surface of gold nanoparticle (GNP) by whispering gallery mode biosensing. Utilizing this scheme, it is furthermore shown that the stoichiometric ratio of GNP attached oligonucleotide species can be controlled by varying the concentration ratio of thiolated oligonucleotides that are used to modify the GNP.

Gold nanoparticles (GNP) are one of the most widely used nanomaterials in chemistry, biology, and medicine, and have been at the forefront of nanotechnology due to their fascinating optical, electronic, and catalytic properties^[1]. GNPs are easily modified by thiol-gold interactions, forming self-assembled layers from a multitude of possible thiolated molecular species, including polymer, oligonucleotide, and peptide^[2]. Among these thiol functionalized GNPs, oligonucleotide-GNP complex has become an important candidate for nanotechnology research due to the designable molecular recognition capability and controllable temperature responsive property. It acts as a popular building block for nanostructured materials^[3], serves as an intracellular gene regulation agent for the control of protein expression in cells^[4], and finds use as a promising DNA-based tool for biosensing^[5]. Moreover, the oligonucleotide-GNP conjugates containing different DNA fragments exhibit more than one recognition sequence to hybridize with complementary strands, which can introduce more diverse functions in nanoparticle applications. For instance, Jwa-Min Nam and coworkers successfully developed PCR-less target DNA amplification method based on two-component oligonucleotide-modified GNPs^[6]. In a recent application, three different fluorescence labeled oligonucleotides binding with GNP act as an accurate nanothermometer with respect to the DNA melting temperature^[7].

Working with multifunctional GNP often requires knowledge on the stoichiometric ratio of the attached oligonucleotides. The most commonly used method for detecting the surface composition of DNA-GNPs is, to the best of our knowledge, the fluorescence-based method described by Linette Demers^[8], which was introduced already in the year 2000. This method, however, can have many drawbacks, mainly due to the use of the fluorescent label. For

example, fluorescence emission can be heavily influenced by a variety of environmental factors, such as pH, temperature, and solvent properties, possibly introducing errors when determining intensity from fluorescence spectra. The method also requires the release of fluorescently labeled oligonucleotides from the nanoparticles before taking fluorescence measurement. Therefore, an effective label-free method is required for determining the stoichiometric ratio between different oligonucleotide species attached to GNPs.

Optical approaches have been developed for the label-free detection of oligonucleotides, among them are whispering gallery (WGM) mode biosensors^[9]. WGM biosensors yield a resonance signal due to the confinement of light by total internal reflection, for example in a ~ 250 μm glass microsphere. WGM-based biosensor systems track the changes in optical resonance frequency or wavelength, and have received tremendous attention because of their large optical quality (Q) factors combined with small optical mode volumes, which result in ultra-high sensitivity for detecting biomolecules^[10]. A WGM biosensor system detects the binding of target molecules^[11] by measuring the resonance wavelength shift caused by small variations of effective refractive index after binding of the target molecules at the microsphere sensor surface. Moreover, WGM sensors have been successfully used in the detection of metal ion concentrations^[12], single nanoparticles^[13], and the conformational changes in biomolecules^[14]. Despite such a variety of applications, there have been no reports on determining stoichiometry, that is to say the relative proportion of molecular species, attached either directly to the sensor surface or attached to the surface of nanoparticles.

Here, we demonstrate the label-free detection of oligonucleotide stoichiometry on multifunctional GNP using a WGM biosensor. The ratiometric detection scheme relies on tracking WGM wavelength shifts upon hybridization of complimentary DNA strands. Our results show that the stoichiometric ratio of two different oligonucleotide species attached to GNP can be determined with high accuracy from the hybridization reaction. Furthermore, utilizing this scheme for multifunctional GNP analysis, we show that the stoichiometric ratio of GNP attached oligonucleotide species can be controlled by varying the concentration ratio of thiolated oligonucleotides that are used to modify the GNP.

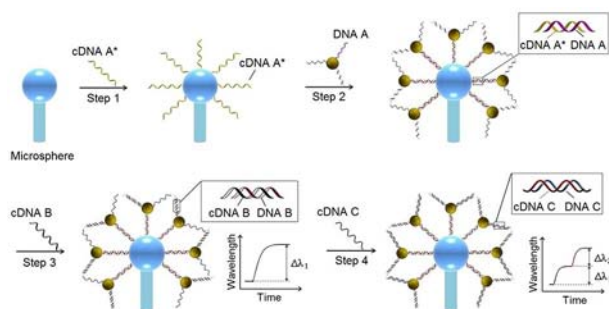


Fig. 1 Schematic illustration of the WGM biosensor measurement for the ratiometric detection of oligonucleotide stoichiometry on multifunctional GNP.

Details of the experimental setup are shown in figure S1. Nine different oligonucleotides (Table S1) were used in our experiments. Among these oligonucleotides, cDNA A, cDNA B, and cDNA C were complementary to DNA A, DNA B, and DNA C respectively. The cDNA A*, cDNA B* and cDNA C* have the same sequences with cDNA A, cDNA B, and cDNA C, but they were modified with biotin at the 5'-end. Multi-oligonucleotide-functional GNPs were modified in solution with three thiolated oligonucleotides with sequences of DNA A, DNA B, and DNA C, where the sequences were unrelated to each other (figure S2). In step one (figure 1), a microsphere was conjugated with cDNA A* through biotin-streptavidin interaction^[15]. We took aliquots from the GNP stock solution and linked those to the WGM sensor via complementary base pairing between DNA A and cDNA A*, see step two. The microsphere was then fixed within a liquid droplet cell on the WGM biosensor system, where a microstirrer was used to homogenize the reaction (figure S1). Upon injection of cDNA B, step three in figure 1, the WGM wavelength showed a red shift owing to the binding of cDNA B with DNA B on the GNP surface. The wavelength shift saturates as the hybridization reaction reaches equilibrium when essentially all complementary oligonucleotides on the GNP surface are hybridized to their complement. In step four, a second WGM wavelength shift is observed upon injection of cDNA C. All complementary oligonucleotides are added to the reaction chamber at 2 μ M final concentrations to ensure that all single stranded oligonucleotides on the GNP surface are bound to their complement in equilibrium.

Since the lengths of cDNA oligonucleotides designed in this study are identical, the magnitude of the WGM wavelength red shift is proportional to the amount of oligonucleotide hybridized to the multifunctional GNPs linked to the WGM microsphere sensor. The stoichiometric ratio of DNA B to DNA C is then estimated from the hybridization signals by dividing the two wavelength shift signals, that is, $\Delta\lambda_1/\Delta\lambda_2$ diagrammed in figure 1. The ratio of DNA A to DNA B or DNA A to DNA C can be estimated in similar fashion, by tethering the multifunctional GNPs from aliquots of our stock solutions to the microsphere modified with cDNA C* or cDNA B*, respectively, and then injecting the complementary strands (cDNA A and cDNA B, or cDNA A and cDNA C).

Prepared multi-oligonucleotide-functional GNP samples were analyzed on a 1% agarose gel by gel electrophoresis (figure 2A). As expected, the bare GNPs remained in the well where they aggregated in $1 \times$ TBE buffer (left lane). The DNA modified GNPs, however, remained solubilized in the TBE buffer and migrated into the gel matrix where they formed a red band (right lane). These results show that the GNPs were successfully modified with oligonucleotides by our thiol reaction^[16].

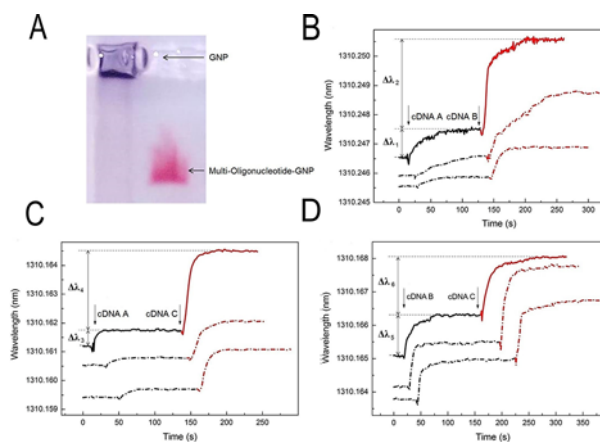


Fig. 2 Ratiometric detection of the stoichiometry of DNA A to DNA B to DNA C oligonucleotides on GNP. (A) 1% agarose gel analysis of GNPs (left lane: bare GNPs control; right lane: multi-oligonucleotide-functionalized GNPs). (B), (C), and (D) show the WGM wavelength shifts $\Delta\lambda$ that were measured and used to calculate the stoichiometry of DNA A to DNA B, DNA A to DNA C, and DNA B to DNA C on the GNP. All the experiments were repeated twice with parallel results shown as dash-dot lines. Black and red parts represent the first and the second oligonucleotides injected to the WGM sensor system. Arrows indicate the injection time points.

The experimental data is shown in figure 2B-D: GNPs modified with thiolated DNAs were conjugated to a microsphere's surface through the DNA (C, B) and cDNA (C, B)* hybridization. A first oligonucleotide was added (cDNA A, cDNA A), figures 2B, C, black part, and the wavelength shift $\Delta\lambda_1$ (1, 3) is observed as the hybridization reaction saturates and reaches equilibrium. The second oligonucleotide (cDNA B, cDNA C) was then added, resulting in a second wavelength red shift $\Delta\lambda_2$ (2, 4) (figures 2B, C, red part). The average wavelength shifts were determined after reaching equilibrium (see figures 2B, C). All experiments were repeated twice. The stoichiometric ratio of DNA B to DNA A was then calculated from $\Delta\lambda_2/\Delta\lambda_1$ with a result of 3.23 ± 0.06 (mean \pm standard deviation), and the stoichiometric ratio of DNA C to DNA A from $\Delta\lambda_4/\Delta\lambda_3$ at 5.06 ± 0.08 . Combining the results of the two experiments, the ratiometric stoichiometry of DNA A to DNA B to DNA C was estimated at 1: 3.23:5.06.

To test validity and accuracy of the WGM ratiometric detection scheme, we next determine the DNA C to DNA B stoichiometry, figure 2D, with a result of DNA C to DNA B stoichiometric ratio of 1.53 ± 0.11 . This experimental result is in good agreement with the predictions from the previous experiments from which we expect a DNA C to DNA B stoichiometric ratio of 1.57, suggesting that the ratiometric detection scheme based on DNA hybridization is accurate with an error of less than 5%.

Next, we use our WGM biosensing method to examine how the concentration ratio of oligonucleotides in the thiol reaction affects the stoichiometric ratio of the surface immobilized oligonucleotides on the GNPs. For this study, 5 kinds of tri-oligonucleotide-modified GNPs were prepared from thiol reactions with the following thiolated oligonucleotide concentration ratios: DNA A to DNA B to DNA C 1:1:1, 1:2:1.5, 1:4:2.5, 1:6:3.5, and 1:8:4.5 respectively. Again, the samples were loaded onto 1% agarose gel to verify successful GNP functionalization, figure S4.

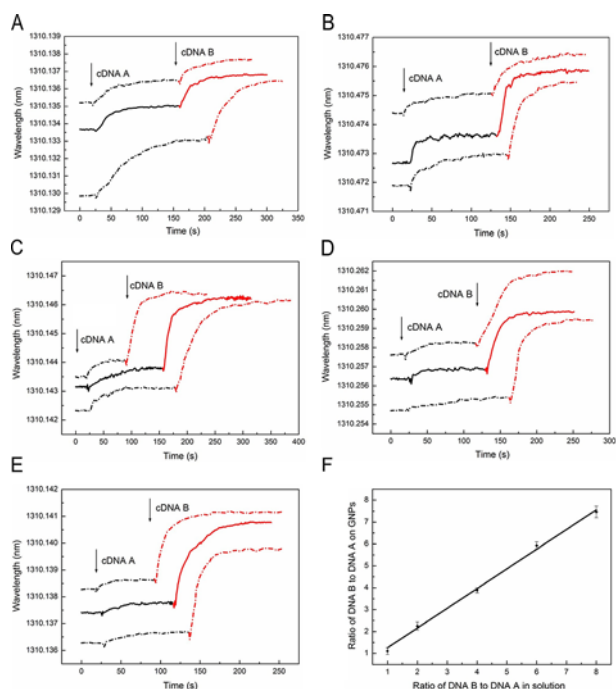


Fig.3 Detection of the relationship between oligonucleotide ratio in solution and on GNP's surface. The solution ratio of DNA B to DNA A were 1:1 (A), 2:1 (B), 4:1 (C), 6:1 (D), and 8:1 (E). (F) DNA A and DNA B loading as a linear function of solution stoichiometry on 15 nm GNPs.

DNA C served as a linker to conjugate to cDNA C* on the microsphere WGM sensor, and we determine the stoichiometric ratio of DNA B and DNA A oligos attached to the GNPs prepared in the five different thiol reactions with varying relative oligonucleotide concentration levels of 1:1, 2:1, 4:1, 6:1, and 8:1 (figure 3A to 3E). All experiments were repeated twice. The stoichiometric ratios of DNA A and DNA B on the GNPs were determined as described before, with results of DNA B to DNA A stoichiometric ratio of 1.10 ± 0.15 (figure 3A), 2.25 ± 0.18 (figure 3B), 3.88 ± 0.12 (figure 3C), 5.93 ± 0.17 (figure 3D), and 7.47 ± 0.26 (figure 3E). Next, we plotted the experimentally determined stoichiometric ratios of oligonucleotides on the GNPs versus the ratio of the concentration of DNA B and A in the thiol reaction, figure 3F. Each point represents the mean value from 3 parallel test results and error bar is the standard deviation. It is seen that a linear relationship was identified with a slope of 0.92, indicating that the surface composition of multi-functional GNPs prepared with a thiol reaction can be controlled by adjusting solution concentrations of oligonucleotides.

Conclusions

We have successfully developed a new and reliable method to ratiometrically determine the stoichiometry of oligonucleotides attached to the surface of GNPs using WGM microsphere biosensors. Furthermore, we showed the application of the WGM biosensor for investigating how concentration ratios of oligonucleotides in a thiol reaction affect the resulting stoichiometry of the oligonucleotides conjugated to the surface of GNP. We find a linear relationship between surface stoichiometry and solution concentration ratio. In summary, our method, having avoided the possible problems resulting from fluorescent molecules, can be applied for ratiometric analysis of more complex system, and may be further developed to provide quantitative data on the absolute number of molecules attached to GNP. As such, our study significantly expands the

application and scope of the WGM technology and points to interesting avenues in the field of nanoparticles based nanotechnologies.

Notes and references

^a Technical Institute of Physics and Chemistry, Chinese Academy of Sciences, Beijing 100190, China.

^b University of Chinese Academy of Sciences, Beijing 100080, China.

^c Laboratory of Nanophotonics & Biosensing, Max Planck Institute for the Science of Light, Erlangen, 91058, Germany. E-mail: frank.vollmer@mpl.mpg.de

^d Division of Biomedical Engineering, Brigham and Women's Hospital, Harvard Medical School, Boston, MA, 02115, USA

[†]This work was supported by Max Planck Society, Germany, NIH grant 1R01GM095906-01 from the National Institutes of General Medical Sciences (NIGMS), USA.

Electronic Supplementary Information (ESI) available: [Experimental setup, Materials and methods, Figure S1, S2, and S3, Table S1]. See DOI: 10.1039/c000000x/.

1. M. Daniel, D. Astruc, *Chem. Rev.*, 2004, **104**, 293.
2. a) P. C. Patel, D. A. Giljohann, D. S. Seferos, C. A. Mirkin, *PNAS.*, 2008, **105**, 17222; b) X. Wang, G. Li, T. Chen, M. Yang, Z. Zhang, T. Wu, H. Chen, *Nano Lett.*, 2008, **8**, 2643.
3. S. Y. Park, A. K. R. Lytton-Jean, B. Lee, S. Weigand, G. C. Schatz, C. A. Mirkin, *Nature*, 2008, **451**, 553.
4. N. L. Rosi, D. A. Giljohann, C. S. Thaxton, A. K. R. Lytton-Jean, M. S. Han, C. A. Mirkin, *Science*, 2006, **312**, 1027.
5. D. Li, A. Wieckowska, I. Willner, *Angew. Chem.*, 2008, **120**, 3991.
6. J-M. Nam, S. I. Stoeva, C. A. Mirkin, *J. Am. Chem. Soc.*, 2004, **126**, 5932.
7. S. Ebrahimi, Y. Akhlaghi, M. Kompany-Zareh, A. Rinnan, *ACS Nano*, 2014, **8**, 10372.
8. L. M. Demers, C. A. Mirkin, R. C. Mucic, R. A. Reynolds, R. L. Letsinger, R. Elghanian, G. Viswanadham, *Anal. Chem.*, 2000, **72**, 5535.
9. a) M. D. Baaske, M. R. Foreman, F. Vollmer, *Nat. Nano.*, 2014, **9**, 933; b) J. D. Suter, I. M. White, H. Zhu, H. Shi, C. W. Caldwell, X. Fan, *Biosens. Bioelectron.*, 2008, **23**, 1003.
10. F. Vollmer, D. Braun, A. Libchaber, M. Khoshshima, I. Teraoka, S. Arnold, *Appl. Phys. Lett.*, 2002, **80**, 4057.
11. J. T. Kindt, M. S. Luchansky, A. J. Qavi, S-H Lee, R. C. Bailey, *Anal. Chem.*, 2013, **85**, 10653.
12. S. Panich, K. A. Wilson, P. Nuttall, C. K. Wood, T. Albrecht, J. B. Edel, *Anal. Chem.*, 2014, **86**, 6299.
13. a) S. K. Ozdemir, J. Zhu, X. Yang, B. Peng, H. Yilmaz, L. He, F. Monifi, S. H. Huang, G. L. Long, L. Yang, *PNAS.*, 2014, **111**, 3836; b) B-B. Li, W. R. Clements, X. C. Yu, K. Shi, Q. Gong, Y. F. Xiao, *PNAS.*, 2014, **111**, 14657; (c) T. Lu, H. Lee, T. Chen, S. Herchak, J. H. Kim, S. E. Fraser, R. C. Flagan, K. Vahala, *PNAS.*, 2011, **108**, 5976.
14. K. A. Wilson, C. A. Finch, P. Anderson, F. Vollmer, J. J. Hickman, *Biomaterials*, 2012, **33**, 225.
15. Y. Wu, D. Y. Zhang, P. Yin, F. Vollmer, *Small*, 2014, **10**, 2067.
16. Y. Kimura, S. Kaneda, T. Fujii, S. Murata, *Electr. Commun. JPN.*, 2013, **96**, 42.